Department of Meteorology

University of Reading

Derivation of an urban materials spectral library through emittance and reflectance spectroscopy

Simone Kotthaus[1,2] | Thomas E. L. Smith[2] | Martin J. Wooster[2,3] | Sue Grimmond[1]

[1]University of Reading, Department of Meteorology; [2]King's College London, Department of Geography; [3]NERC National Centre for Earth Observation, UK

Motivation

- Urban surfaces are composed of a vast variety of natural and anthropogenic materials. The latter are not yet well represented in existing spectral libraries (Heiden et al. 2007)
- Radiative properties → impact surface radiation balance → impacts boundary layer climates
- Thermal remote sensing is increasingly used in urban areas
- Advances are expected from new hyperspectral sensors covering long-wave infrared region (Hook et al. 2013)
- Algorithms for temperature-emissivity separation need to be improved for complex urban settings
- Materials with high reflectance are regarded as a key part of a strategy for climate mitigation (Akbari et al. 2012)
- Spectral response in both short- and long-wave spectral regions can aid mapping of urban surface materials (e.g. to provide/improve model parameterisations)

Materials

Impervious materials collected from across a European city centre (London):

- Natural and composite impervious materials (Table 1, photos)
- Natural materials are key constituents of the composite materials (e.g. granite aggregate in asphalt)
- 74 samples analysed:
  - 10 material classes (Table 1) according to usage
  - New, used and weathered

Table 1: Material classes (class ID) of samples of impervious urban materials in London. N=number of samples in each (sub-) class.

Material class	Sub-class	N
Quartzite (X)	Quartzite conglomerate	3
Stone (S)	Sandstone	3
	Limestone	2
Granite (G)	Granite	5
Asphalt (A)	Road asphalt	9
	Asphalt roofing paper	1
Concrete/ cement (C)	Concrete	4
	Cement	3
Brick (B)	Clay brick	7
	Cement brick	7
Roofing shingle (L)	Roofing shingle	4
Roofing tiles (R)	Ceramic roofing tile	7
	Concrete roofing tile	5
Metal (Z)	Metal	5
	Metal, painted	3
PVC (V)	PVC	6

Impervious urban materials

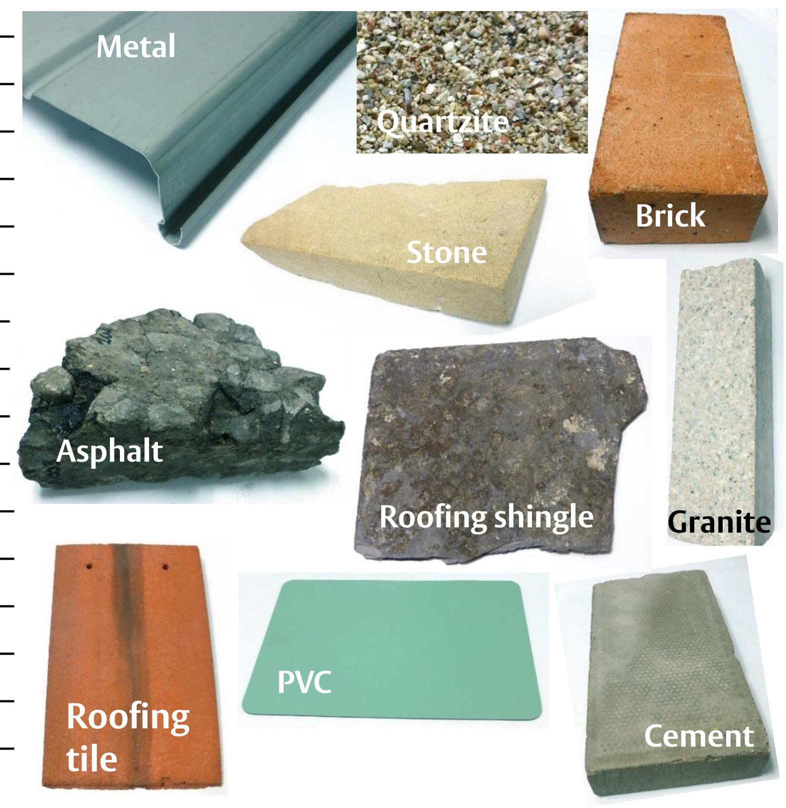

Methods

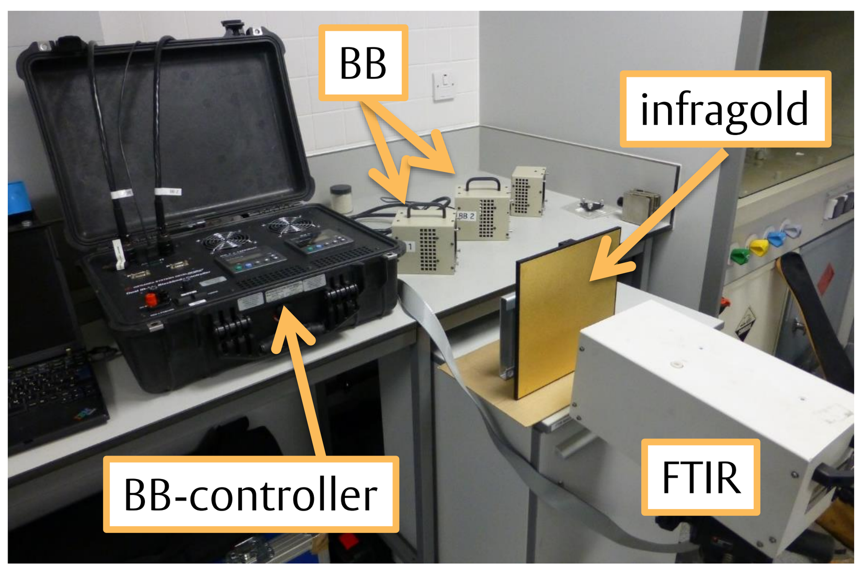

Figure 1: Measurement setup for LWIR observations in the laboratory with the MIDAC FTIR system, blackbody (BB) radiation sources and infragold reference panel.

- Field spectroscopy methods covering two spectral regions:
  a) visible to short-wave infrared (VIS-SWIR) 300-2500 nm with a *SVC* HR-1024 spectrometer
  b) long-wave infrared (LWIR) 8-14 µm with a *MIDAC* M2000 FTIR spectrometer (Figure 1)
- Radiometric calibration of FTIR observations based on measurements of two flat-plate IR-2100 Blackbody Systems (*Infrared Systems Development*).
- Incoming ambient radiance was quantified using a gold reference panel (*Infragold*).
- Processing/quality control: Kotthaus et al. (2014)
- Emissivity retrieval: blackbody fit method (Kahle and Alley 1992) for laboratory observations and Iterative Spectrally Smooth Temperature-Emissivity Separation (ISSTES, Borel 1998) outdoors.
- Linearity of the FTIR system evaluated by testing a range of temperatures (Figure 2, Figure 3).
- Temporal and spatial stability of blackbodies (BB) found to be ± 0.2 W m^{-2} µm sr^{-1}.
- Lab measurements: material samples heated well above room temperature (50-60°C). Most accurate radiometric calibration with BB temperatures set to closely bracket target temperature (Figure 3).

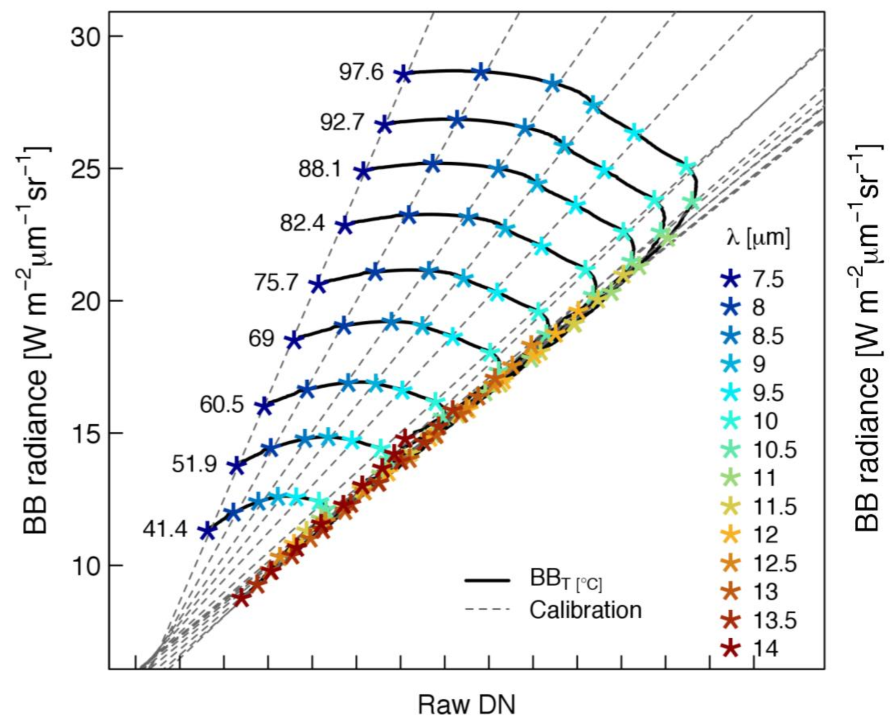

Figure 2: Spectral radiance calculated for a flat plate blackbody (BB) system with ε = 0.96 at different temperatures T (labelled [°C]) displayed against Raw DN (digital numbers) recorded by the MIDAC FTIR system when observing the same BB source. Linear relations, that define the radiometric calibration between raw DN and spectral radiance, are shown for a series of selected wavelengths (dashed lines).

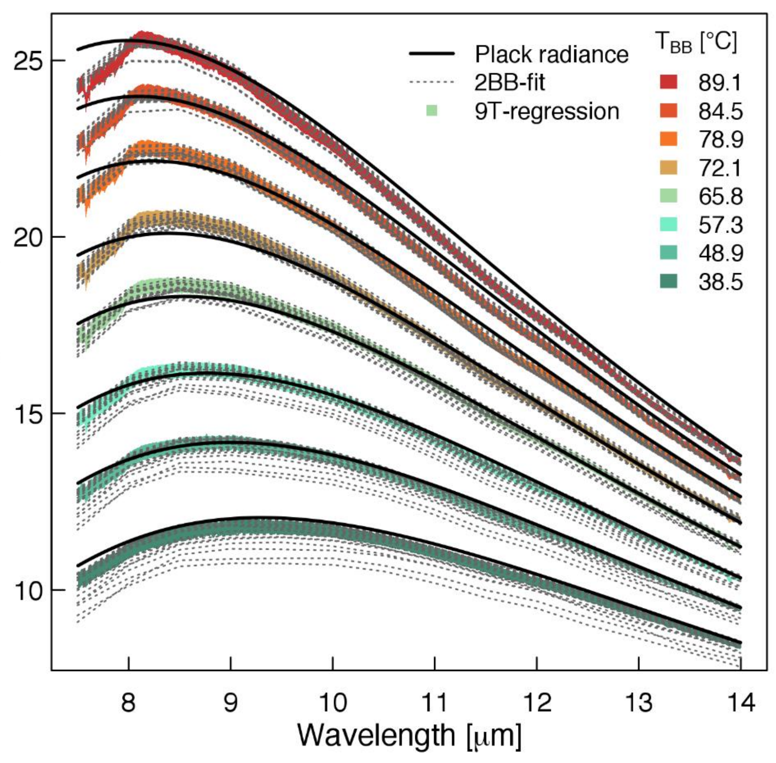

Figure 3: Blackbody spectral radiance of an independent radiation source at different temperatures (T_{BB}), calibrated using the observations of the flat plate black bodies at nine temperatures (9T) (Figure 2): (shaded area) spectral radiance calculated via the application of the linear calibration relations derived through all nine BB temperature observations ± spectral root mean square error, (dashed lines) spectral radiance calculated from linear calibration relations derived through observations at 20 combinations of two selected BB temperatures (2BB-fit). For reference: (solid line) expected values according to the Planck function (ε = 0.96).

Results (Kotthaus et al. 2014)

- SLUM agrees well with spectra from existing spectral libraries (e.g. MODIS Wan et al. 1994, USGS Clark et al. 2007, ASTER Baldridge et al. 2009).
- Many impervious urban materials have more distinct absorption (and reststrahlen) features in the LWIR compared to the VIS-SWIR (Figure 4).
- New, anthropogenic construction materials (e.g. PVC) still rare in spectral libraries and only few metals available; PVC shows diverse signatures in VIR-SWIR reflectance (Figure 4, left).
- Metals vary across all wavelength studied.
- Weathering and finish clearly impact short-wave reflectance (especially for metals).
- Estimated broadband emissivity and albedo reveal no clear relation between response in the two wavelength regions.
- Aggregate materials dominant in many composite materials such as concrete or asphalt.

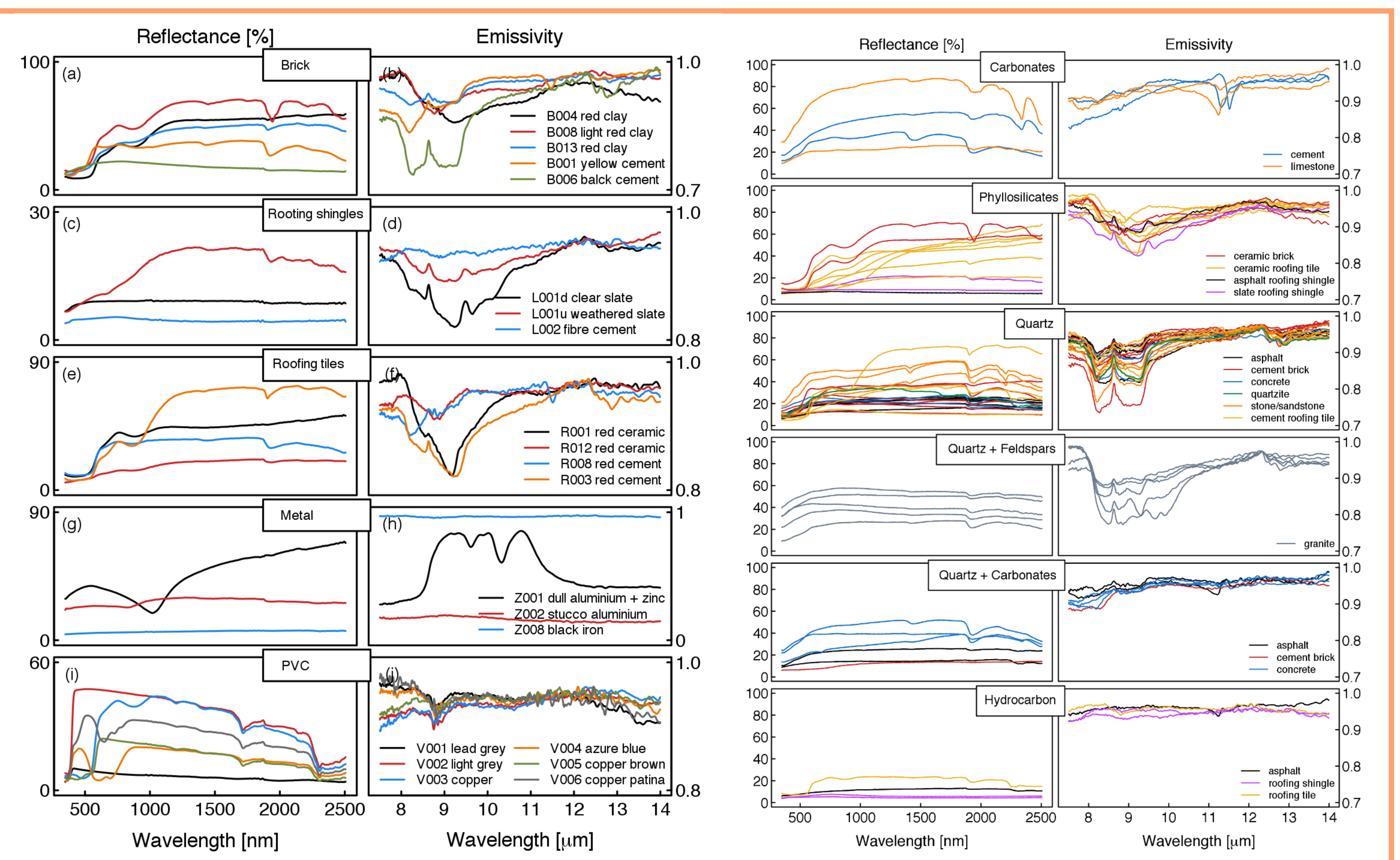

Figure 4: Absolute VIS-SWIR reflectance and LWIR emissivity spectra determined using laboratory-based spectroscopy observations for (left) five of the ten SLUM classes (Table 1) and (right) impervious urban materials whose long-wave radiative response is dominated by carbonates, clay minerals (phyllosilicates), quartz minerals, quartz plus feldspar, quartz plus carbonate or hydrocarbons.

Materials split into six categories (Figure 4, right) according to LWIR response:
Carbonates: dominated by calcium carbonate in both regions
Phyllosilicates: spectra reveal superposition of a range of clay minerals
Quartz: distinct quartz doublet in LWIR, no consistent features in SW region
Quartz + feldspars: clear silica signatures in LWIR, mostly featureless in VIS-SWIR
Quartz + Carbonates: only weak quartz features remain due to superposition
Hydrocarbon: high absorption in VIS-SWIR and LWIR; no absorption signatures

LUMA Spectral Library of impervious Urban Materials (SLUM) available on **www.met.reading.ac.uk/micromet/LUMA/SLUM.html**

Conclusions

- Most construction materials can be classified according to the dominant minerals → multi-/hyperspectral LWIR data provide more detailed information compared to VIS-SWIR.
- No clear relation apparent between broadband response in LWIR and VIS-SWIR.
- Broadband generally:
  - $0.89 > \varepsilon > 0.97$
  - some metals with $0.16 < \varepsilon < 0.89$
  - albedo very diverse with $0.05 < \alpha < 0.68$
- Radiative response of both metals and PVC is not yet sufficiently understood. More research is required to characterise their role as urban surface components.

Contact information

- Department of Meteorology, University of Reading, Whiteknights, RG6 6AH
- s.kotthaus@reading.ac.uk | www.met.reading.ac.uk/micromet/LUMA/SLUM.html

Acknowledgements

This study was funded by EUFP7 Grant agreement no. 211345 (BRIDGE), NERC ClearfLo (NE/H003231/1), EPSRC (EP/I00159X/1, EP/I00159X/2) Materials Innovation Hub and KCL; URBANFLUXES is co-financed by "HORIZON 2020" EU Framework Programme. Supported by NERC FSF (Natural and Environmental Research Council Field Spectroscopy Facility) we thank Alasdair MacArthur and Chris MacLellan for their technical advice on the operation of both the SVC HR-1024 and the MIDAC FTIR. Some of the material samples were kindly provided by Paul Baldwin at ARUP. We thank Jeremy Bourdon and Margot Myers for their help in gathering material samples and Dr Bruce Main, Dr Trevor Blackall, Grace Healy, Oscar Finnemore, John Mustchin and Will Morrison for their assistance when performing the measurements. We thank Simon Hook at NASA JPL for providing the Ottawa sand sample.

References

Akbari H, H Damon Matthews, D Seto, 2012: The long-term effect of increasing the albedo of urban areas. *Environ. Res. Lett.*, 7, 024004.
Baldridge AM, SJ Hook, CI Grove, G Rivera, 2009: The ASTER spectral library version 2.0. *Remote Sens. Environ.*, 113, 711–715.
Borel CC, 1998: Surface emissivity and temperature retrieval for a hyperspectral sensor. *IGARSS 98 Sensing and Managing the Environment*, Vol. 1 IEEE Intern. Geoscience & Remote Sensing Symp, No98CH36174.
Clark RN, GA Swayze, R Wise, E Livo, T Hoefen, SJ Kokaly, R, Sutley, 2007: USGS digital spectral library splib06a. *U.S. Geological Survey, Digital Data Series 231*. http://speclab.cr.usgs.gov/spectral.lib06/.
Heiden U, K Segl, S Roessner, H Kaufmann 2007: Determination of robust spectral features for identification of urban surface materials in hyperspectral remote sensing data. *Remote Sens. Environ.*, 111, 537–552.
Hook, SJ, WR Johnson, MJ Abrams, 2013: NASA's Hyperspectral Thermal Emission Spectrometer (HyTES), in: Kuenzer, C, S, Dech (Eds.), *Thermal Infrared Remote Sensing*. Springer Netherlands, pp. 93–115.
Kahle AB, RE Alley, 1992: Separation of temperature and emittance in remotely sensed radiance measurements. *Remote Sens. Environ.*, 42, 107–111.
Kotthaus S, TEL Smith, MJ Wooster, CSB Grimmond, 2014: Derivation of an urban materials spectral library through emittance and reflectance spectroscopy, *ISPRS J Photogramm Remote Sens*, 94, 194–212 .
Wan Z, D Ng, J Dozier, 1994: Spectral emissivity measurements of land-surface materials and related radiative transfer simulations. *Adv. Space Res.*, 14, 91–94.